

Aerofoil at low speeds with Gurney flaps

L. Brown and A. Filippone

Department of Mechanical

Aerospace, Manufacturing Engineering, UMIST

Manchester, UK

ABSTRACT

This paper reviews the research on Gurney flaps and related high lift trailing edge devices. It investigates aerofoil performances at Reynolds numbers $Re \approx 10^5$ and below, both with the clean configuration and various Gurney flap sizes. The device height is optimised, and a semi-empirical formula linking flap height to free stream speed and aerofoil chord is proposed. The analysis shows that the optimal size of the device is always below the boundary-layer thickness at the trailing edge. Discussion of results includes analysis of hysteresis loops occurring in the L/D performances. These are mostly due to large changes in drag and small changes in lift, which occur when the aerofoil is restored to the reference angle of attack.

1.0 INTRODUCTION

The Gurney flap is a vertical tab added to the trailing edge on the pressure side of a wing. Car racer Dan Gurney is credited as the inventor in the early 1970s, although no patent could be granted. The idea (probably due to plain intuition, turned out to be much older, and was patented as a 'Zaparka Flap' in 1935, after Frank Zaparka, the originator⁽¹⁾). This flap was never tested and it never came to the attention of the aerospace industry, until Gurney's aerodynamicist Gary Wheeler at the Douglas Aircraft Company, Long Beach, introduced it to Robert Liebeck, who tested it in the wind-tunnel⁽²⁾. The main difficulty of the original flap was that it hinged on a structurally weak point of the wing (e.g. the trailing edge). Also, it was envisioned as a high-lift device in the climb segment, to be retracted

during cruise, because of the drag penalty. Thus, the concept was labelled as inferior to the split flap, which hinged on a stronger point of the wing.

The Douglas Corporation was impressed by the results, and started an experimental campaign in the high speed flight regime. A 0.5% chord, full-span Gurney flap on the wind-tunnel model of the DC-10 created a 20% increase in total aircraft lift, and practically no change in total aircraft drag during the second segment climb configuration. Obviously, such an increase in lift instigates an increase in lift-induced drag. The aircraft drag being constant was deemed a spectacular result.

Over the years the device has often shown itself to improve glide ratios, L/D , of aircraft wings in a variety of applications including light aircraft, such as the Cessna 208B stretched Caravan, although the application was meant to increase the C_{Lmax} only. On some western helicopters (for example, Boeing AH-64 Apache) Gurney flaps are fitted on the horizontal inverted wing to improve performance during the high-powered climb, when the wings tend to stall. It is also used on many helicopter vertical tails, to increase the force produced by a horizontal stabiliser (for example, the Sikorsky S-76).

Wheeler⁽³⁾ reports more subtle applications. For example, when fuel costs rose steeply during the Arab oil embargoes in the middle 1970s, some airlines suggested to cruise the DC-10 at a lower speed – but at the same altitude. Lower cruise speed required two degrees more angle of attack, and caused more fuselage drag. The Gurney flap was seen as a winning concept in that case, because it moved the centre of lift aft, and shifted the $C_L - \alpha$ curve upwards.

At that point the aerospace industry (particularly the Douglas Corp. and Lockheed) made efforts to find some derivative of the Gurney flap that would be patentable. The next step was called the Trailing Edge Wedge, which offered some structural advantages. It lacked the performances of the Gurney flap, but wind-tunnel tests soon proved it could simply be made larger until it would become nearly identical in function.

The first idea of the trailing edge wedge is apparently due to Irv Culver (the one time director of Lockheed's Skunk Works). In the 1980s he had designed a high-performance hang glider (Swing Wing) that featured a large balsa wood trailing-edge wedge. Culver's resale of the plans put the device into the public domain, and no patent could be issued.

Douglas, however, were able to narrow it to cover high speed applications where it would be used to enhance the performance of supercritical aerofoils (such as Whitcomb's) by adding more trailing edge camber without altering the contours of the suction side of the aerofoil. The 'Trailing Edge Wedge' was then named the 'Divergent Trailing Edge' (DTE), Refs 4-6. Part of the very low drag seen during second segment climb on the DC-10 wind-tunnel model, was from reduced fuselage lift and drag, since that unavoidable source of inefficient lift was reduced – traded for more efficient wing lift. The DTE was used in the new aircraft MD-11 (late 1980s), with a somewhat smaller base height.

Whilst the DTE has structural advantages when used on high-speed wings, the Gurney flap actually outperforms the DTE from an aerodynamic point of view. For transonic aircraft, as long as it is kept small, the Gurney flap can even be used to suppress flutter (using so called micro-flaps or trailing edge effectors, patented by Lockheed⁽⁷⁾). At lower speeds the flap can be used to tune the span-wise lift distribution, or to alter the aerodynamic twist on an existing aircraft.

Initially it was thought that the flap worked due to an effective increase in wing camber that it produced. Most people (including Liebeck and Wheeler) still consider this to be true. However, it has now been established that the Gurney flap produces a pair of counter-rotating vortices behind itself (Liebeck himself had anticipated their existence). These vortices produce circulation that works in addition to the circulation of the main wing, hence overall circulation and lift is increased. These vortices are rather unsteady, and have oscillatory characteristics at low Reynolds numbers (like a von Kármán street). They have been visualised in a recent work by Sims-Williams *et al*⁽⁸⁾. Therefore, the flap's performances must be considered as a time average.

Lift enhancement without drag penalties is a must in aeronautical applications. Increases in glide ratios with a relatively small drag penalty are not acceptable, although in some instances small drag reduction is possible. In the Breguet equation the range scales with L/D (in first approximation). Increased L/D with a drag penalty, though, requires additional engine power, that can be only provided at the expense of increased specific fuel consumption (SFC). This, on turns, would tend to decrease the aircraft range. The effect of the device is in general quite dubious, because it is not straightforward to determine the increased SFC as a function of the drag penalty. Extremely low drag wing applications (like NASA's Solar Flying Wing) are one of those cases where drag increase is routinely true and Gurney flap applications are not appropriate.

The Gurney flap promotes two other flow characteristics that are beneficial to performance. The sharp 90° corner increases the velocity close to the trailing edge on the suction surface, thus reducing the boundary-layer thickness and helping to delay trailing edge stall. It also increases the positive pressure close to the trailing edge on the pressure side of the wing, which helps to further increase the force generated.

Over the years more impetus has gone into similar high lift devices, which are mechanically simple, have no moving parts, require no particular maintenance and can be retrofitted. These include serrated trailing edges with saw-tooth configuration^(9,10), and wedge shaped flaps for attachment to or near the trailing edge⁽¹¹⁾.

In racecar applications regulations on wing size often results in huge a Gurney flap sometimes with heights up to 10% chord. Formula 1 cars often use very large Gurney flaps on slow tracks where the drag penalty is irrelevant, but in many cases optimal compromise between downforce gain and L/D penalties seem to be a height in the order of several percent.

Regarding the optimisation of the device height, there is more to it than just finding the optimum L/D trade-offs from a 2D aerofoil wind-tunnel test. For example, in aerospace applications the Gurney flap may turn out to provide such a large increase in cruise C_L , that a substantial reduction in wing area may be possible. This obviously introduces compounding efficiencies from weight reduction, reduced wetted area, etc. Consequently, in practice an actual aircraft may benefit from a larger Gurney flap than one might first think from simply looking at 2D aerofoil test data.

When aircraft cruise drag becomes important, it usually turns out that 1% of local aerofoil chord is a good starting point. No detectable cruise drag penalty was found during the DC-10 flight tests, although the application exists only over the outboard two metre (or about five feet) of flap span. (That was done to avoid placing the non-flying tail in a downwash that would have created unwanted trim drag.) They certainly have to be sized smaller than the boundary-layer thickness to avoid trailing edge icing.

The technical literature has recently addressed the flap's performances in the high Reynolds numbers range, $Re \approx 10^6$, for aeronautical applications^(10,13). Liebeck⁽²⁾ concluded that flap heights of about 1% chord were optimal from the point of view of increased glide ratio L/D , and that a flap size of 2% or more contributed to a drag rise.

Giguère *et al*⁽¹⁴⁾, were the first to investigate the flow scaling problem by systematic testing of the aerofoil LA203A at $Re \approx 10^6$. They presented results showing 'uncertainty in the experimental data'. Yet, they were able to assess that the optimal flap height scales with the boundary-layer thickness, δ . Results plotted against the aerofoil's angle of attack show a decreasing flap height.

Other relevant research includes applications to helicopter rotors⁽¹⁵⁾, to delta wings⁽¹⁶⁾ and wind turbines⁽¹⁷⁾, or coupled with vortex generators⁽¹⁸⁾. More recently, several tests were conducted by Richter and Rosemann⁽¹⁹⁾ at transonic speeds with various combinations of pure Gurney flaps and divergent trailing edge shapes.

In this study we will focus on the optimisation of the Gurney's height in the very low speed regime ($Re \approx 10^5$ and below), to find an analytical expression linking the optimal height to the free stream velocity and aerofoil's chord. The low Reynolds number range is a cause of hysteresis loops on the glide ratio, which are attributed to different flow conditions during flow separation and re-attachment. These are studied in detail.

2.0 EXPERIMENTAL SET-UP

The wing was of rectangular planform with a span $b = 0.457\text{m}$ (equal to the wind-tunnel width), and a constant chord $c = 0.154\text{m}$, corresponding to an aspect-ratio of 2.94, Fig. 1. The maximum thickness was 10mm at $x/c = 0.15$, and the maximum relative thickness to chord ratio was $t/c = 0.065$.

The wing was built from a single piece of balsa wood and had a steel rod that extruded from the right-hand side in order for it to be clamped horizontally onto the force balance. The surface of the aerofoil was sealed with diluted PVA glue and spray-painted with waterproof black gloss paint; this enabled oil flow visualisation to be performed.

The wind-tunnel was an open jet low speed facility (Plint blower tunnel). The test section was a square 0.457m \times 0.457m, and had a length of 1.2m. Boundary-layer correction is achieved by using corner fillets that extend along the contraction cone and the working section. This ensures a uniform longitudinal pressure in the test section.

The velocity range in the experiments discussed in this paper was 4.1ms⁻¹ to 15.0ms⁻¹. The aerofoil chord was used as a length scale for the Reynolds number (Re 42,000-160,000).

2.1 Flow quality

Due to the tunnel having an open circuit design, flow quality was of lower quality in comparison to the more expensive closed circuit design. Our estimates were the following:

- Mean turbulence level in test section = 0.7% rms.
- Velocity distribution across test section = $\pm 1.0\%$

A low Reynolds number increases the extent of laminar flow. A turbulence level of 0.35% would cause a 50% reduction in the transitional Reynolds number, as reported by Schubauer and Skramstad⁽²⁰⁾. This can be particularly critical in the low speed flight regimes. We have visualised the flow on the suction side of the wing at different angles of attack on the plain aerofoil. The effect of the Gurney flap is negligible, as this is mounted on the opposite side. Figure 2 shows the turbulent transition with spanwise changes created by turbulence and small surface irregularities. (Flow is from left to right.) The smooth flow on the left is the laminar boundary-layer region. This is followed by a transitional region with laminar separation, a turbulent re-attachment line and a turbulent boundary-layer.

2.2 Force and velocity measurements

The aerodynamic forces on the aerofoil are measured using a balance. The balance fitted to the wind-tunnel is a three-component pyramidal balance that enables the lift, drag and pitching moments to be calculated. The strain gages of the balance are connected to a calibrated digital readout that displays values of drag, fore and aft forces. From these values, the 'zero velocity' readings need to be subtracted in order to give a change in force rather than the absolute force. The overall lift force can be found from the summation of the fore and aft readings. The drag, in particular, is a global force, and therefore it was not possible to investigate the spanwise effects (these would require the use of the momentum method).

3.0 ESTIMATION OF ERRORS AND UNCERTAINTIES

In order to verify that the results are accurate to within reasonable limits it is necessary to analyse the potential errors and uncertainties within the experiments.

This is done by first estimating the errors and uncertainties of the experimental measurements. These are: Vernier scale used for aerofoil length measurements: $\pm 0.1\text{mm}$; Micrometre used for the Gurney flap measurements: $\pm 0.01\text{mm}$; Manometre fluid level height: $\pm 0.1\text{mm}$; Air density value: $\pm 0.01\text{kg/m}^3$; Incidence measurement on balance: ± 0.2 ; Balance force value (aft, fore and drag) on digital display: $\pm 0.005\text{N}$.

These values can be used to estimate errors in additional calculated values such as the aerofoils surface area and total balance forces: Error in lift force (aft + fore): $\pm 0.01\text{N}$; error in drag force: $\pm 0.005\text{N}$.

All of these errors are absolute and therefore they do not depend on any other factors and remain constant for all experimental situations. However, when estimating the error in values such as the free stream velocity and Reynolds number, a constant absolute error cannot be calculated, and therefore a percentage error is required.

The percentage error in free stream velocity was calculated from the manometer height $h = \pm 0.1\text{mm}$ and air density $\rho = 1.225 \pm 0.01\text{kgm}^{-3}$. For any given value of free stream velocity, a maximum and a minimum possible value can also be calculated. This gives a possible velocity range for any given calculated velocity. This velocity range is then converted into a percentage range. This data decreases with the increasing wind speed. The estimated percentage error at an operating velocity of 6.32ms^{-1} is $\pm 2.4\%$, or $\pm 0.152\text{ms}^{-1}$, if converted back into an absolute error. The same analysis can be completed for the Reynolds number calculations. In this case, the percentage error of the free stream velocity is already known and



Figure 1. Aerofoil with Gurney flap in wind-tunnel test section.

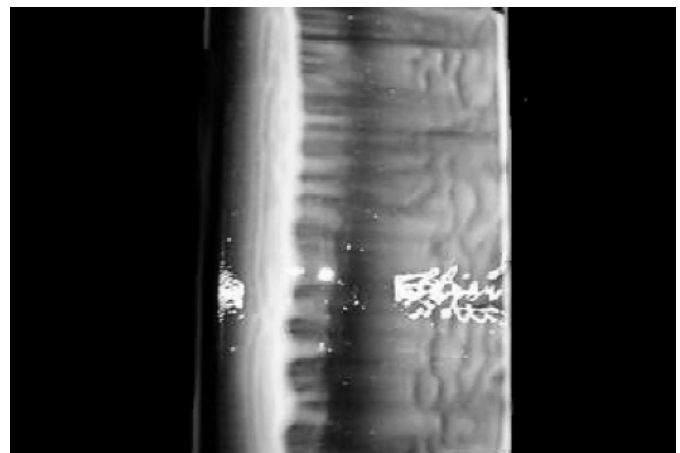


Figure 2. Flow visualisation on the pressure side of the aerofoil, $\alpha = 5^\circ$, $Re = 65,000$.

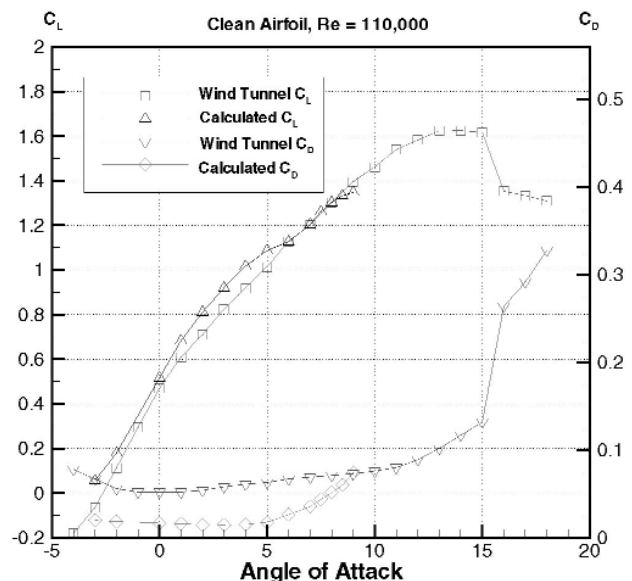


Figure 3. Comparison between calculations and wind-tunnel data for the clean aerofoil, $Re = 110,000$.

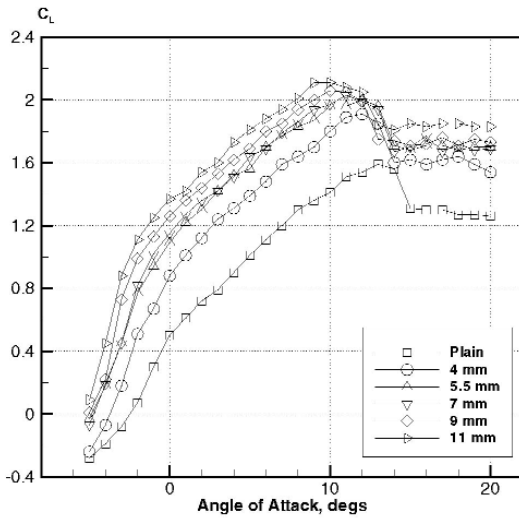


Figure 4. Lift curve as a function of Gurney flap height, Re = 110,000.

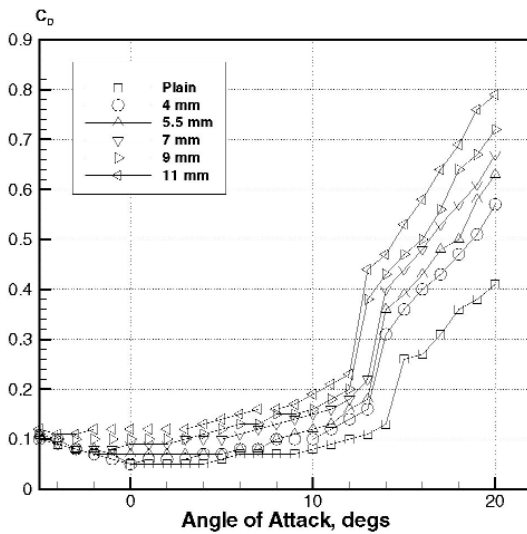


Figure 5. Drag curve as a function of Gurney flap height, Re = 110,000.

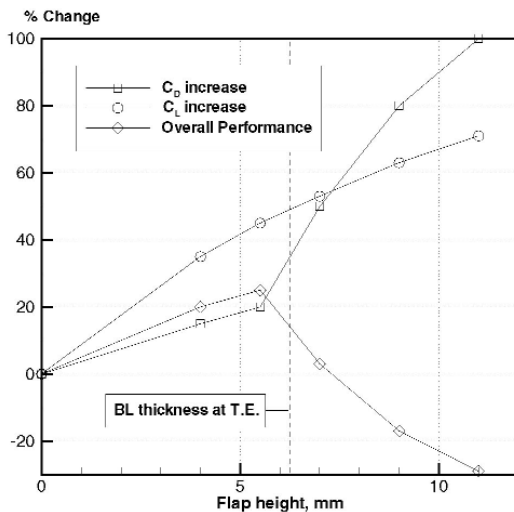


Figure 6. Lift and drag increase as a function of Gurney flap height, Re = 110,000.

therefore this combines with the error in the measurement of x . At $Re = 65,000$ we have an estimated percentage error of $\pm 3\%$, or $\pm 1,950$ in absolute terms. The error is less than 5% , and can therefore be considered as an acceptable experimental error. It is now possible to calculate an absolute error for both the C_L and C_D . These are dependent on the free stream velocity, with the uncertainty decreasing at higher velocities.

The errors in these values are large, particularly at low Reynolds numbers. This is because the C_L and C_D have a velocity squared term, hence the velocity error undergoes a multiplication effect. The absolute errors of the lift and drag coefficients for each experimental Reynolds number are: at $Re = 65,000$, $C_L = \pm 0.047$, $C_D = \pm 0.007$; at $Re = 109,000$, $C_L = \pm 0.010$, $C_D = \pm 0.002$. With the clean aerofoil at $Re = 42,000$ we found a fairly large error on both lift and drag: $C_L = \pm 0.220$, $C_D = \pm 0.030$, a result not within an acceptable level.

It can therefore be seen that the absolute error of the lower Reynolds numbers experiments is significantly greater than the error at slightly higher Reynolds numbers. This explains the large oscillations seen on Fig. 10 for the curve representing a Reynolds number of $65,000$ (more noisy curves – not shown here – were obtained at $Re = 42,000$).

Two further errors that also need to be considered are the effects of solid and wake blockage. Both of them have the effect of increasing the aerofoils drag in comparison to what it would experience in an unbounded flow. Several complex methods exist for calculating the two blockage effects, however a simple approximation is given by Pope⁽²¹⁾ as:

$$\% \text{ Error} = \frac{1}{4} \times \frac{\text{model frontal area}}{\text{test section area}} \times 100 \quad \dots (1)$$

which resolved becomes 0.6% .

It can therefore be seen that the tunnel blockage error is small in comparison to the other experimental errors and can therefore be assumed negligible. The error is also constant for all experiments, and will therefore not affect any ‘change in drag’ values that were seen in the results.

4.0 GURNEY FLAP ANALYSIS

For the Reynolds number experiments only subtle changes in the aerofoils performance characteristics were observed, most notably at angles close to the stall angle. However, it can be seen that in comparison to a plain aerofoil, Gurney flaps give a significant variation in both the lift and drag characteristics over the complete range of incidences investigated ($\alpha = -5$ to 20°).

In order to test the approximation of some of our experimental data, we have carried out some calculations with the program Xfoil⁽²²⁻²³⁾ at the largest Reynolds number. The calculations were performed on the clean aerofoil section, and are shown in Fig. 3. Free transition was assumed with a value of $N_{crit} = 9$ in the e^N method (appropriate to the wind-tunnel turbulence conditions). The data that it was possible to obtain were limited to incidences $\alpha < 9^\circ$. The C_L is close to the experimental data, except for an excess of lift created by a too large separation bubble, although we must take into account small three-dimensional effects and local imperfections (Fig. 2). The C_D is underestimated by a substantial amount (right scale of the graphic). No reliable theoretical data could be obtained at $Re = 65,000$ and below.

The results of the Gurney flap experiments are shown in Fig. 4 (lift curves) and Fig. 5 (drag curves) at $Re = 110,000$. The experiments were carried out from the lowest incidence to the highest, with step changes operated when the flow was considered steady. The corresponding changes in lift, drag, and glide ratio for the different flap heights used is summarized in Fig. 6.

The Gurney flap has a consistent effect on the lift slope at negative incidences, but generates an upward shift in the C_L axis for the complete range of incidence, including after stall. It can be seen that the increase in lift is proportional to the size of the Gurney flap, with the

11mm ($h/c = 0.071$) Gurney flap producing the largest lift increase for any given incidence and the greatest $C_{Lmax} = 2.10$. A notable feature of the Gurney flap lift curves is that even after reaching stall, the aerofoils with Gurney flaps still produce a lift coefficient equal to or greater than that of the plain aerofoil. The increase in the lift coefficient is also coupled with an increase in the drag coefficient. Figure. 5 shows that at angles less than the stall angle, the 4mm ($h/c = 0.026$) and 5.5mm ($h/c = 0.036$) flaps both have similar drag coefficients, being approximately 120% that of the plain aerofoil drag. For the 7mm flap, the drag rise increases up to approximately 150% that of the plain aerofoil. For further increases in flap height, the drag increase remains approximately in proportion to the height increase of the flap.

While the C_D increases with all the flaps tested, the C_L grows faster with the smaller flap sizes. This leads to an optimal size from the point of view of L/D after which further increases in size are detrimental to the aerofoil performances.

In order to fully understand the Gurney flap results it is necessary to estimate the boundary-layer thickness at the trailing edge. As a first approximation (certainly valid for this aerofoils at low incidences), we have used the expressions giving the boundary-layer thickness on a flat plate. Based on a value of local Reynolds number, the laminar boundary-layer thickness at any chord-wise position x is given by Ref. (24):

$$\delta_{99\%} \text{ (lam)} = \frac{5 \cdot 00 x}{\sqrt{\text{Re}_x}} \quad \dots (2)$$

For turbulent flow this thickness can be derived from Prandtl's seventh root law for a velocity profile:

$$\delta_{99\%} \text{ (trb)} = \frac{0 \cdot 383 x}{\sqrt[5]{\text{Re}_x}} \quad \dots (3)$$

For a flat plate operating at $\text{Re} = 100,000$ the corresponding boundary-layer quantities are $\delta = 2.37\text{mm}$ (laminar flow) and $\delta = 5.75\text{mm}$ (turbulent flow). At $\text{Re} 65,000$ we have, respectively, $\delta = 0.75\text{mm}$ and $\delta = 6.26\text{mm}$.

For situations where C_{Lmax} is the principal design criterium, such as in an aircraft landing situation, the drag rise is not problematic, and can actually help to further decelerate the aircraft. In this situation, the largest possible flaps should be used. However, if Gurney flaps are to be used for cruise applications then they can only be an effective addition if the lift to drag ratio is increased above that of the plain aerofoil, i.e. the gain in lift must be greater than the gain in drag. Figure 7 shows the lift and drag increase due to each Gurney flap in terms of a percentage increase from the plain aerofoil values at $\text{Re} = 110,000$ (from data of Figs 4 and 5).

From the study of Fig. 6 it can be seen that the optimum lift to drag ratio occurs when the Gurney flap height is slightly below the trailing edge boundary-layer thickness. This can be noted from the dashed line that represents the percentage difference between the lift increase and the drag increase.

It can therefore be proposed that when using Gurney flaps to improve the performance in a cruising situation, the flap height should be restricted to 90% of that of the trailing edge boundary-layer total thickness. This leads to an equation that relates the optimum Gurney flap height h (in mm) to the chord length and the average cruising free stream Reynolds number:

$$h_{opt} = 0.9 \cdot \delta_{99\%} \cdot 10^3 \quad \dots (4)$$

or

$$h_{opt} = \left(0.9 \cdot \frac{0.383 x}{\sqrt[5]{\text{Re}_x}} \right) \cdot 10^3 \quad \dots (5)$$

However, the free stream Reynolds number is itself a function of the chord length, and so the equation can be simplified to a function of only the chord length and the average velocity:

$$h_{opt} = 0.9 \cdot \frac{0.383 x}{\sqrt[5]{Uc/v}} \cdot 10^3 \quad \dots (6)$$

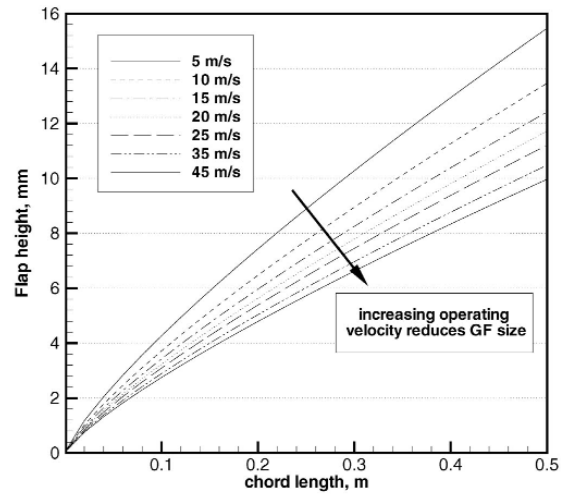


Figure 7. Gurney flap optimisation chart.

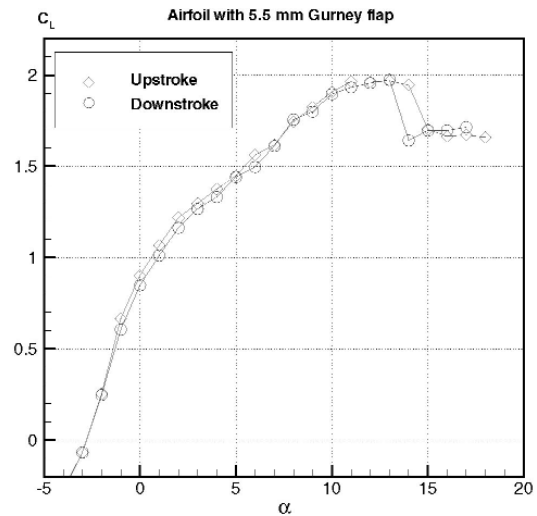


Figure 8. C_L for aerofoil with 5.5mm Gurney flap, $\text{Re} = 65,000$.

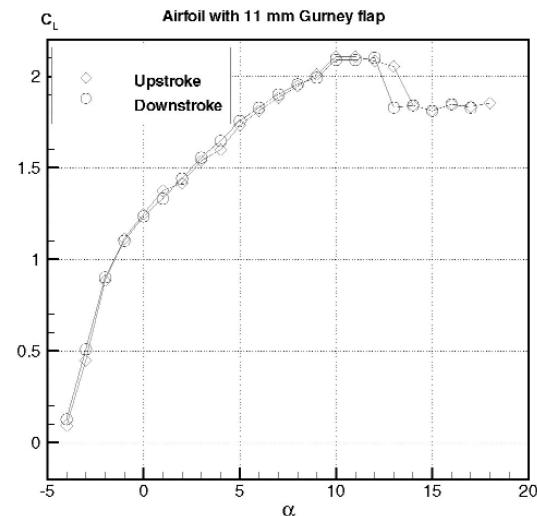


Figure 9. C_L for aerofoil with 11mm Gurney flap, $\text{Re} = 65,000$.

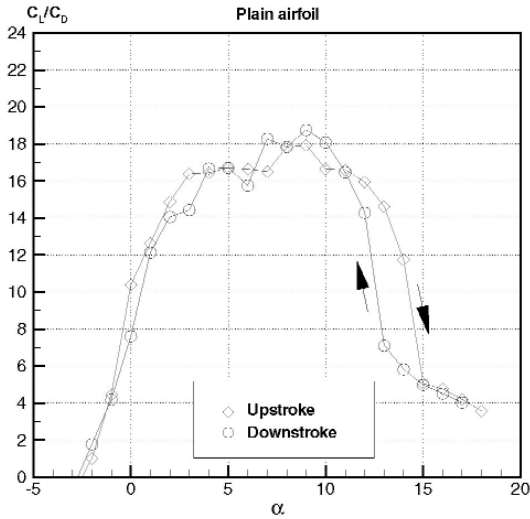


Figure 10. Glide ratio for clean airfoil, $Re = 65,000$.

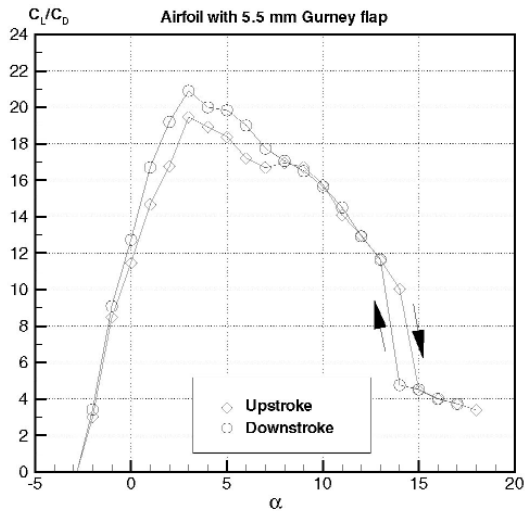


Figure 11. Glide ratio for airfoil with 5.5mm Gurney flap, $Re = 65,000$.

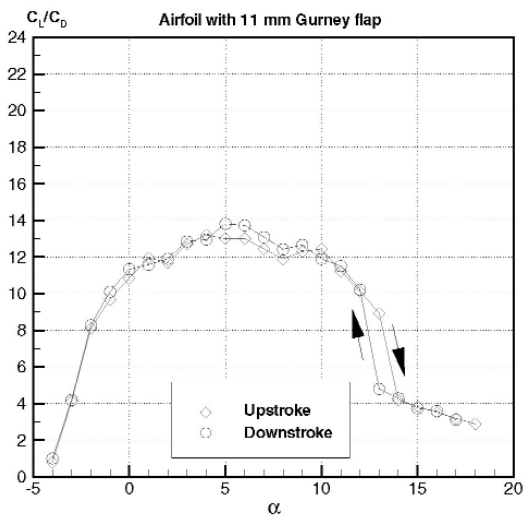


Figure 12. Glide ratio for airfoil with 11mm Gurney flap, $Re = 65,000$.

$$h_{opt} = 0.9 \cdot 0.383^{0.8} c \left(\frac{v}{U} \right)^{0.2} \cdot 10^3 \quad \dots (7)$$

where the chord c is given in metres and the velocity U is given in ms^{-1} . Using the value $\nu = 1.455 \cdot 10^{-5} \text{m}^2/\text{s}$ for the kinematic viscosity, we finally find a relationship for the optimum Gurney flap height in mm as a function of the aerofoil chord and free stream velocity:

$$h_{opt} = 37.155 \left(\frac{c^{0.8}}{U^{0.2}} \right) \cdot 10^3 \quad \dots (8)$$

It is now possible to apply this equation to any given situation with the optimum flap height quickly being found. Figure 7 shows the equation in a graphical form, with each line representing an average operating velocity.

Taking as an example a racing car rear wing, the chord length is approximately 0.30m and the average velocity on a typical circuit is $u = 150 \text{km/h}$ (or about 40ms^{-1}). From the graph, this shows that the optimum Gurney flap height is $h = 6.8 \text{mm}$. Note that for motor sport applications, this optimisation procedure enables the Gurney flaps to be optimised for each individual circuit based on the circuits average speed. For example, the chart of Fig. 7 shows that a larger flap would be required on a street circuit where the speeds are slower compared to an oval track where the average velocity is higher. Moving surfaces are currently forbidden in all major formula, however if these were to become permitted then an interesting development would be to design 'active Gurney flaps'. These would be capable of changing their height depending on the car's real time velocity, and would therefore maintain the optimum performance at all positions on the circuit.

5.0 ANALYSIS OF HYSTERESIS EFFECTS

In the Reynolds number range tested the oil flow visualisations showed that a short bubble is present on the aerofoil's upper surface and that stall occurs due to the separation bubble becoming unable to reattach and leading edge separation occurring.

At low Reynolds numbers, a major effect of separation bubbles is the occurrence of hysteresis loops within the lift curve slope. The separation bubbles cause the lift curve slope to be different when incidence is increasing to when it is decreasing, and hence a 'loop' is formed. A typical example of this phenomenon is shown in Figs 8 and 9, both at $Re = 65,000$. This phenomenon is quite sensitive to the geometric characteristics of the aerofoil (besides the Reynolds number), and it does not always occur.

There are two types of hysteresis loop, the 'short bubble clockwise hysteresis' and the 'long bubble anticlockwise hysteresis' (Selig *et al*)⁽²⁵⁾. Short bubble hysteresis occurs at the stall angle and is caused by the short separation bubble that remains attached until the stall angle is reached. After stall, as the aerofoil incidence is decreased, the flow is unable to reattach until a lower angle is reached than the initial stall angle. This then forms a clockwise loop on the lift curve graph, within which the lift can have two possible values depending on whether incidence is increasing or decreasing. Long bubble hysteresis can occur at any incidence between the zero-lift angle and stall. As incidence is increased, the long bubble will lengthen and move towards the leading edge, with a corresponding increase in drag and decrease in performance. As the angle is increased further, the long bubble suddenly breaks down into a short bubble and the aerofoil returns to its original lift and drag values. Hence, lift is suddenly increased with the gradient of the lift curve slope also increasing. As the incidence is decreased, the short bubble does not burst back into a long bubble until a lower incidence is reached, hence a loop is formed. Long bubbles hysteresis can be avoided if the Reynolds number is increased. Long bubble anticlockwise hysteresis can be seen to occur at 7° and short bubble clockwise hysteresis occurs at the stall angle of 15° .

The effect of the bubble on the drag coefficient is more difficult to assess, but hysteresis loops exist also in this case and tend to grow bigger at the low Reynolds numbers around the point of static stall. As a consequence, the glide ratio hysteresis loop will locally amplify, as shown in Figs. 10 to 15 for the clean aerofoil and for the aerofoil with optimal and sub-optimal Gurney flap. The results show that the size of the loop depends strongly on the Reynolds number.

In practical situations hysteresis loops are unfavourable, particularly if the aerofoil is in a dynamic situation close to stall. For example when an aircraft is landing, it may be one degree below the stall angle with a lift value close to C_{Lmax} . If turbulence were then to temporarily increase the incidence above the stall angle, short bubble hysteresis would cause the lift to return to a value much lower than it was originally which is undesirable in terms of aircraft control.

6.0 CONCLUDING REMARKS

Very low Reynolds number performances of a thin high lift aerofoil with and without Gurney flaps have been investigated. It was found that Gurney flaps produce an upward shift in the lift coefficient that is approximately proportional to the flap height. At angles below stall, the drag increase to the Gurney flap with a height less than the trailing edge boundary-layer is less than 20%. For flaps of larger height, or for an aerofoil that has stalled, the drag increase can typically become up to twice that of the plain aerofoil. The maximum lift to drag ratio occurs when the flap height is about 90% that of the trailing edge boundary-layer thickness. This leads to an optimum height equation that enables the efficient optimisation of any constant-chord aerofoil. The experiments have shown that as long as the height remains less than the thickness of the boundary-layer at the trailing edge, the additional drag will be negligible, which is coherent with other data available in the technical literature for high Reynolds number flows. The flap, therefore, can be applied to a number of low Reynolds number systems, including gliders, micro air vehicles, wind turbines, etc.

ACKNOWLEDGEMENTS

The authors would like to thank Gary Wheeler for reporting on the history of the Gurney flap from his own experience, and for commenting of the drag characteristics of the device.

REFERENCES

1. ZAPARKA, F. United States Patent RE-19, 412 (reissue), Jan 1935.
2. LIEBECK, R.H. Design of subsonic aerofoils for high lift. *J Aircr*, September 1978, **15**, (9), pp 547-561.
3. WHEELER, G. Private communication, March 2002.
4. HENNE, P.G. and GREG, R.D. Divergent trailing-edge aerofoil. United States Patent No 4,858,852 (on the Internet at <http://www.uspto.gov>), August 1989.
5. HENNE, P.G. and GREG, R.D. A new aerofoil design concept. *J Aircr*, **28**, (5), pp 300-311, October 1991. (Also AIAA Paper 89-2201, 1989).
6. HENNE, P.A. *Innovation With Computational Fluid Dynamics: The Divergent Trailing-Edge Aerofoil*, **125**, Progress in Aeronautics and Astronautics, Chapter 8. AIAA, 1991.
7. WAINFAN, B. Micro flap trailing edge device for an aircraft wing. United States Patent No 4,867,396 (on the Internet at <http://www.uspto.gov>), September 1989.
8. SIMS-WILLIAMS, D.B. WHITE, A.J. and DOMINY, R.G. Gurney flap aerodynamic unsteadiness. *Sports Engineering*, Nov 1999, **4**, (2), pp 221-234.
9. VIJGEN, P.M.H.W., HOWARD, F.G., BUSHNELL, D.M. and HOLMES, B.J. Serrated trailing edges for improving lift and drag characteristics of lifting surfaces. United States Patent No 5,088,665 (on the Internet at <http://www.uspto.gov>), February 1992.
10. VAN DAM, C.P. YEN D.T. and VIJGEN, P.M.H.W. Gurney flap experiments on aerofoils and wings, March 1999, *J Aircr*, **36**, (2), pp 484-486.

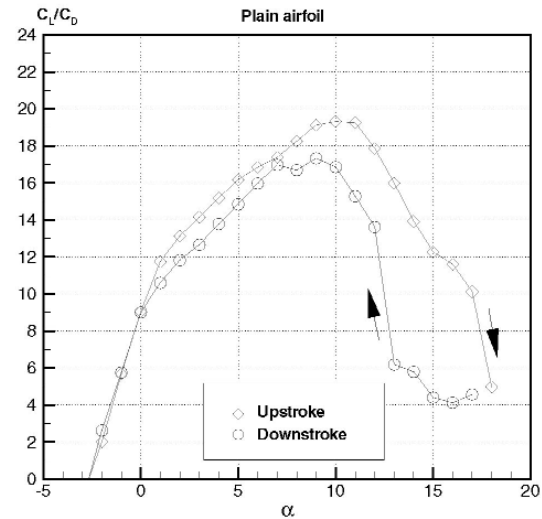


Figure 13. Glide ratio for clean aerofoil, $Re = 110,000$.

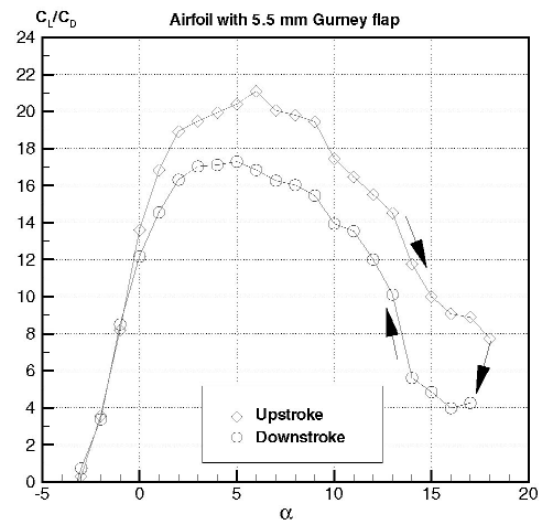


Figure 14. Glide ratio for aerofoil with 5.5mm Gurney flap, $Re = 110,000$

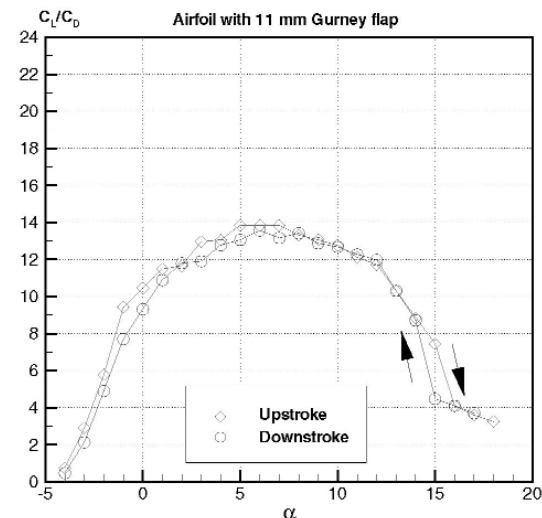


Figure 15. Glide ratio for aerofoil with 11mm Gurney flap, $Re = 110,000$.

11. BOYD, J.A. Trailing edge device for an aerofoil. United States Patent No 4,542,868 (on the Internet at <http://www.uspto.gov>), September 1985.
12. KATS, J. and DYKSTRA, L. Study of an open-wheel racing car's rear-wing aerodynamics. In SAE International Congress and Exposition, SAE Paper 890600, Feb. 1989, Detroit, MI.
13. MYOSE, R., PAPADAKIS, M. and HERON, I. Gurney flap experiments on aerofoils, wings, and reflection plane models. *J Aircr*, March 1998, **35**, (2), pp 206-211.
14. GIGUERE, P., LEMAY, J. and DUMAS, G. Gurney flap scaling for optimum lift-to-drag ratio. *AIAA J*, December 1997, **35**, (12), pp 1888-1890.
15. KENTFIELD, J.A.C. The potential of Gurney flaps for improving the aerodynamic performance of helicopter rotors. AIAA Paper 93-4883, 1993.
16. BUCHHOLZ, M.D. and TSO, J. J. Lift augmentation on delta wing with leading-edge fences and Gurney flap. *J Aircr*, December 2000, **37**, (6), pp 1050-1057.
17. BAO, N., MA, H. and YE, Z. Experimental study of wind turbine power augmentation using aerofoil flaps, including the Gurney flap. *Wind Engineering*, **24**, (1), pp 25-34, January 2000.
18. STORMS, B.S. AND JANG, C.S. Lift enhancement of an aerofoil using a Gurney flap and vortex generators. *J Aircr*, May 1994, **31**, (3), pp 542-547.
19. RICHTER, H. and ROSEMANN, H. Experimental investigation of trailing-edge devices at transonic speeds. In Proceedings of the Royal Aeronautical Society Aerodynamics Research Conference, April 2001, pp 27.1-27.9, London.
20. SCHUBAUER, G.B. and SKRAMSTAD, H.K. Laminar-boundary-layer oscillations and transition on a flat plate. NACA Report 909, 1948.
21. POPE, A. and RAE, W.H. *Low-Speed wind-tunnel Testing* John Wiley, 1984.
22. DRELA, M. XFOIL: An analysis and design system for low Reynolds number aerofoils, in lecture notes in engineering No 54. Springer Verlag, 1989.
23. DRELA, M. Low-Reynolds number aerofoil design for the MIT Daedalus prototype: A case study. *J Aircr*, August 1988, **25**, (8), pp 724-732.
24. HOUGHTON, E.L. and CARPENTER, P.W. *Aerodynamics for Engineering Students*. Arnold Publ, 1993, London.
25. SELIG, M.S., GUGLIELMO, J.J., BROEREN, A.P. and GIGUERE, P. Experiments on aerofoils at low Reynolds numbers. AIAA Paper 96-0062, 1996.